



## UvA-DARE (Digital Academic Repository)

### Electronic structure of K-intercalated tris-hydroxyquinoline alimunium (Alq3) studied by photoemission spectroscopy

Schwieger, T.; Peisert, H.; Knupfer, M.; Golden, M.S.; Fink, J.

**Publication date**

2001

**Published in**

Physical Review B

[Link to publication](#)

**Citation for published version (APA):**

Schwieger, T., Peisert, H., Knupfer, M., Golden, M. S., & Fink, J. (2001). Electronic structure of K-intercalated tris-hydroxyquinoline alimunium (Alq3) studied by photoemission spectroscopy. *Physical Review B*, 63, 165104.

**General rights**

It is not permitted to download or to forward/distribute the text or part of it without the consent of the author(s) and/or copyright holder(s), other than for strictly personal, individual use, unless the work is under an open content license (like Creative Commons).

**Disclaimer/Complaints regulations**

If you believe that digital publication of certain material infringes any of your rights or (privacy) interests, please let the Library know, stating your reasons. In case of a legitimate complaint, the Library will make the material inaccessible and/or remove it from the website. Please Ask the Library: <https://uba.uva.nl/en/contact>, or a letter to: Library of the University of Amsterdam, Secretariat, Singel 425, 1012 WP Amsterdam, The Netherlands. You will be contacted as soon as possible.

# Electronic structure of K-intercalated 8-tris-hydroxyquinoline aluminum studied by photoemission spectroscopy

T. Schwieger, H. Peisert, M. Knupfer, M. S. Golden, and J. Fink

*Institut für Festkörper- und Werkstofforschung Dresden, D-01171 Dresden, Germany*

(Received 27 June 2000; published 3 April 2001)

We have studied the electronic structure of potassium-intercalated 8-tris-hydroxyquinoline aluminum using valence-band and core-level photoemission spectroscopy. It is shown that low K intercalation leads to a rigid shift of the chemical potential to higher energies. This shift allows the determination of a lower limit of the transport energy gap of pristine 8-tris-hydroxyquinoline aluminum of 3.05 eV. This number is significantly larger than the gap measured using absorption techniques that shows that the optical excitation is excitonic. The energy levels of 8-tris-hydroxyquinoline aluminum are considerably modified upon further intercalation that is assigned to a combination of structural relaxation and the impact of the alkali counter ions.

DOI: 10.1103/PhysRevB.63.165104

PACS number(s): 71.20.Rv, 79.60.-i

## I. INTRODUCTION

Recently, there has been growing interest in the properties of organic semiconductors and their application in various devices such as organic light emitting diodes.<sup>1</sup> Alq<sub>3</sub> (8-tris-hydroxyquinoline aluminum) is one of the organic materials that is often used as an electron transport and emission layer in such devices and thus can be regarded as a model substance for the understanding of the functionality of these devices. Figure 1 schematically shows the molecular structure of Alq<sub>3</sub>. A detailed knowledge of the electronic structure and the injection as well as the transport of charge carriers in the organic devices is essential for a microscopic understanding of the different properties of the device components.

Intercalation with potassium represents one way to study negatively charged Alq<sub>3</sub> and thus can provide information about its properties in an electron-transport layer. We therefore studied the electronic structure of K-intercalated Alq<sub>3</sub> at various K concentrations up to three potassium atoms per Alq<sub>3</sub> molecule. Previously, various investigations on metal/Alq<sub>3</sub> interfaces have been carried out (Ca, Mg, Ga).<sup>2-4</sup> These contributions mainly deal with the change of Fermi and/or vacuum levels due to the interface formation, which is important for the determination of injection barriers in organic devices. Johansson *et al.*<sup>5</sup> recently discussed the results of a joint theoretical and spectroscopic study of the occupied-electronic states in K- and Li-intercalated Alq<sub>3</sub>. Curioni and Andreoni<sup>6</sup> have presented an overview of the results of their discrete Fourier transform (DFT) calculations on metal (Li, Al, Ca)-Alq<sub>3</sub> complexes and Treusch *et al.*<sup>7</sup> published an analysis of the unoccupied states of pristine Alq<sub>3</sub> using x-ray absorption spectroscopy. The results presented in this contribution aim at a deeper insight into the electronic structure of K-intercalated Alq<sub>3</sub>. We discuss the changes of the valence band electronic structure, the distribution of the additional charge on the molecules and the changes in the work function with intercalation.

## II. EXPERIMENT

Our studies have been carried out using ultraviolet photoemission spectroscopy (UPS) and x-ray photoemission spec-

troscopy (XPS). For both UPS and XPS a commercial PHI 5600 system was used, which was equipped with an unmonochromatized He-discharge lamp providing photons with 21.2 eV for UPS and a monochromatized Al K $\alpha$  x-ray source (1486.6 eV photons) for XPS. The UPS spectra have been corrected for the contributions from He I $\beta$  and He I $\gamma$  radiation. The total energy resolution of the spectrometer was determined by analyzing the width of a Au Fermi edge to be 100 meV (UPS) and 350 meV (XPS), respectively. In order to obtain thin films, Alq<sub>3</sub> was evaporated in a preparation chamber at a base pressure of  $3 \times 10^{-10}$  onto a clean, argon-sputtered gold foil. After the Alq<sub>3</sub> deposition the sample was transferred to the analysis chamber (base pressure  $1 \times 10^{-10}$ ), where the UPS and XPS measurements were carried out. The thickness of the respective Alq<sub>3</sub> film was determined to be 7 nm by monitoring the attenuation of the intensity of the Au 4f photoemission peak before and after the deposition. We used the formula by Seah and Dench<sup>8</sup> for organic molecules to calculate the mean free path length of electrons in Alq<sub>3</sub> and arrived at 34.3 Å for electrons with a kinetic energy of 1402.6 eV (Au 4f<sub>7/2</sub>). In order to intercalate the films, we evaporated potassium with a commercial SAES potassium getter source. The potassium concentration in the Alq<sub>3</sub> films was derived from a comparison of the rela-

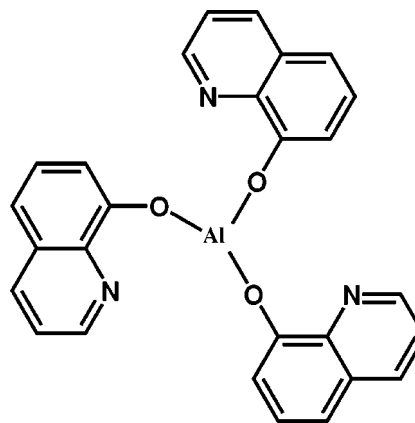


FIG. 1. Schematic representation of the molecular structure of Alq<sub>3</sub>.

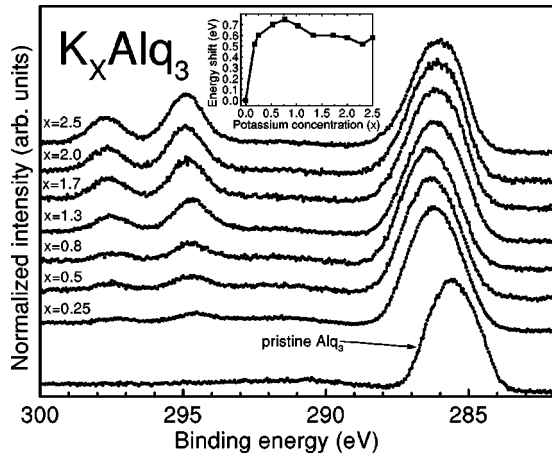


FIG. 2. Evolution of the C  $1s$  and K  $2p$  core levels with increasing potassium intercalation of  $\text{Alq}_3$ . The inset shows the energy shift of the C  $1s$  structure versus increasing potassium content of the sample.

tive intensities of the K  $2p$  and the C  $1s$ , N  $1s$  as well as O  $1s$  core-level intensities. As sensitivity factors we used 1.3 for K  $2p$ , 0.296 for C  $1s$ , 0.477 for N  $1s$ , and 0.711 for O  $1s$ , which take the spectrometer sensitivity into consideration.<sup>9</sup> Taking into account the uncertainty of these factors and other sources of deviation from the ideal conditions, one arrives at an error of the intercalation level of about 15%. The work function of the films was extracted from the linear extrapolation of the low-energy cutoff after applying a bias of 5 eV to the sample that allows all photoexcited electrons to leave the sample. For calibration purposes we measured the work function of gold to be 5.15 eV, which is in good agreement with literature values.<sup>10</sup> All film preparation steps and the measurements themselves were carried out at room temperature.

### III. RESULTS AND DISCUSSION

Intercalation with potassium results in negatively charged,  $n$ -type doped- $\text{Alq}_3$  molecules. In a simple approximation, one might expect the additional electron to occupy the LUMO (lowest unoccupied molecular orbital) of  $\text{Alq}_3$ . Theoretical investigations predict this LUMO to be concentrated on the pyridyl side of the  $\text{Alq}_3$  ligands with the main contributions to the LUMO arising from the carbon and nitrogen atoms.<sup>11</sup> In the following, we first discuss our results from the core-level studies as a function of intercalation before we turn to the valence-band features.

#### A. Core-level spectroscopy

We have measured the O  $1s$ , N  $1s$ , K  $2p$ , C  $1s$ , and Al  $2p$  core-level photoemission spectra of  $\text{K}_x\text{Alq}_3$ . In Fig. 2 the evolution of the C  $1s$  and the K  $2p$  core levels with increasing potassium intercalation is shown. The C  $1s$  peak of pristine  $\text{Alq}_3$  is a broad feature situated at 285.6 eV binding energy (BE) with a linewidth of 1.9 eV. We attribute the linewidth to the presence of inequivalent carbon sites in the  $\text{Alq}_3$  molecule. The corresponding fine structure of the C  $1s$

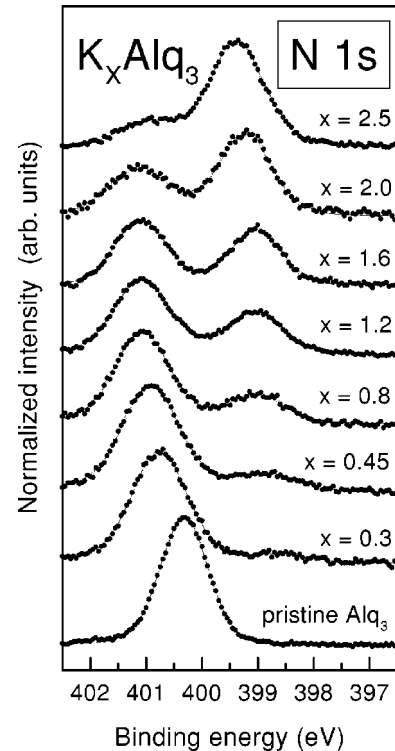


FIG. 3. N  $1s$  core level of potassium intercalation of  $\text{Alq}_3$  as a function of potassium intercalation.

peak cannot be resolved. The K  $2p$  spin-orbit doublet appears at a binding energy (294.8 eV and 297.6 eV) that is consistent with other intercalated  $\pi$  conjugated systems such as the fullerides.<sup>12</sup> This shows that the potassium atoms really transfer their outer  $s$  electron to the  $\text{Alq}_3$  molecules. No vertical gradient in the distribution of the potassium atoms in the  $\text{Alq}_3$  film could be observed when changing the emission angle of the photoelectrons. With increasing potassium concentration we observe a shift of 0.7 eV of the C  $1s$  structure to higher binding energies until a concentration of 0.8 potassium atoms per  $\text{Alq}_3$  molecule is reached. At higher potassium concentrations we find a slight backshift peak maximum to lower binding energies (see inset Fig. 2) that might be related to a change of the underlying C  $1s$  fine structure. This will be discussed in more detail below.

In Fig. 3 the evolution of the N  $1s$  core-level spectra with increasing potassium intercalation is plotted. In the case of pristine  $\text{Alq}_3$  a single line at a binding energy of 400.4 eV is visible, consistent with only one nitrogen site per quinoline ligand. Intercalation with potassium leads to an appearance of a second component at 2.0 eV lower BE. This means that the new component results from an N site that is more negatively charged than that leading to the original N  $1s$  peak. In addition, a broadening of the original N  $1s$  line of approximately 0.15 eV can be observed with intercalation that is most probably caused by intercalation-induced inhomogeneity in the film. The formation of the second component is connected with a decrease of spectral weight of the original N  $1s$  structure. Both the decrease of the original peak and the increase of the new component scale with the potassium concentration in the sample up to a potassium concentration of

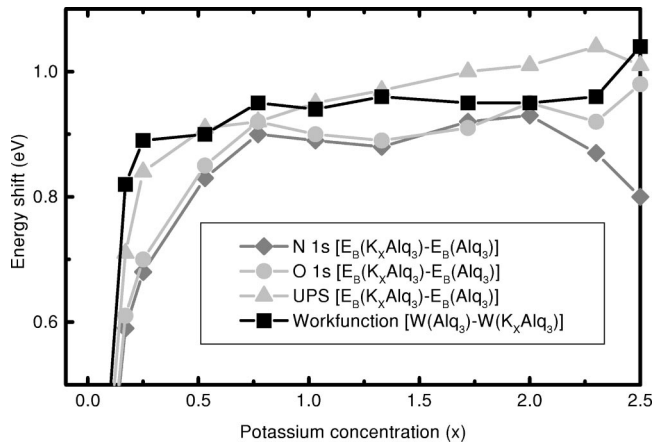


FIG. 4. Energy shift of the peak position of the  $\text{Alq}_3$  N  $1s$  and O  $1s$  core levels, the main features of the valence band and the work function of the sample. Since the work function decreases with increasing potassium concentration, we draw the negative shift of the work function in order to compare the data.  $E_B$  denotes the binding energy of the photoemission features and  $W$  the work function.

$x = 2.5$  ( $\text{K}_x\text{Alq}_3$ ). Beyond this degree of intercalation we observe a low-energy component in the O  $1s$  core-level spectra (not shown) that indicates a surface contamination of the sample as a consequence of surface oxidation. The formation of oxide species on the surface for  $x$  larger than approximately 2.5 suggests that the maximal intercalation level is  $x = 3$ .

The second component in the N  $1s$  core-level spectra is a clear sign for a change of the chemical surrounding of the nitrogen site in  $\text{Alq}_3$  caused by doping of the molecules. This demonstrates that the former LUMO of  $\text{Alq}_3$  that becomes occupied with doping is partly derived from nitrogen  $2p$  states, confirming the calculations of Curioni *et al.*<sup>11</sup> The original N  $1s$  line vanishes when the potassium concentration reaches one potassium atom per quinoline ligand of the  $\text{Alq}_3$  molecule. Additionally the binding energy of the N  $1s$  features increases with increasing intercalation up to  $x = 0.8$  and then stays constant at 0.85 eV BE higher than in the case of pristine  $\text{Alq}_3$ . This will be discussed in detail later.

In Fig. 4 we depict the energy shifts of the N  $1s$  and O  $1s$  core levels together with the shift of the main valence band features and the work function of the corresponding film. The work function drops about 0.9 eV at low intercalation and remains constant above  $x = 0.8$  while the core level and valence band binding energies increase by the same amount. Note that for comparison we show in Fig. 4 the negative change of the work function. Since all energy shifts shown in Fig. 4 agree quantitatively, we assign them to a variation of the energy position of the chemical potential as a function of intercalation. In pristine  $\text{Alq}_3$  the chemical potential lies within the energy gap between the HOMO (highest occupied molecular orbital) and the LUMO. Intercalation then leads to a pinning of the chemical potential at the LUMO of pristine  $\text{Alq}_3$ . Higher doping fills the LUMO with more electrons but does not change the position of the chemical potential sig-

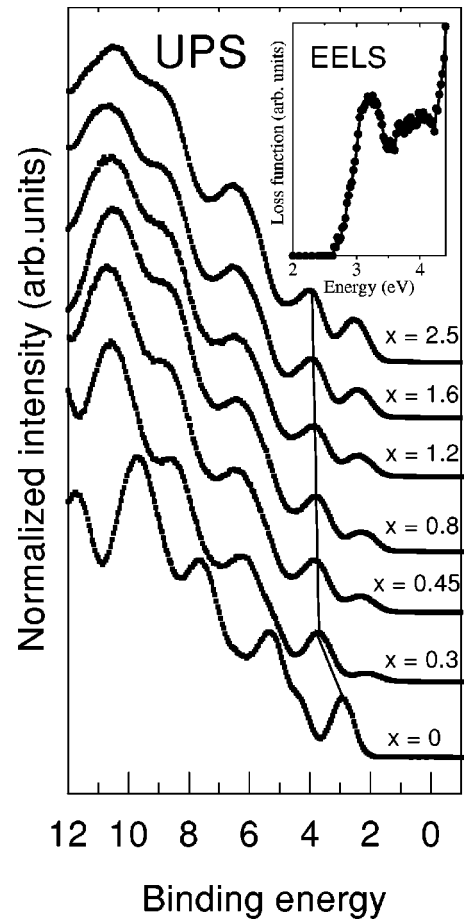


FIG. 5. Valence-band photoemission spectra of  $\text{Alq}_3$  at various potassium concentrations. The line is a guide for the eye to point out the evolution of the first main feature of the valence band. The inset shows the loss function of pristine  $\text{Alq}_3$  obtained by electron energy-loss spectroscopy in transmission.

nificantly. This additionally means that the ionization potential for all electronic levels remains unchanged upon intercalation. We note that the changes in BE observed in Fig. 2 for the C  $1s$  core level are slightly different from what has been discussed above as the C  $1s$  core-level binding energy decreases at higher intercalation levels. We attribute this difference to variations of the underlying fine structure of the C  $1s$  peak as a result of doping as is more clearly illustrated for the N  $1s$  core-level data shown in Fig. 3. This again indicates that both the carbon and nitrogen  $2p$  orbitals contribute to the molecular states near the energy gap of  $\text{Alq}_3$ . The fact that the fine structure changes of the C  $1s$  core level is not resolved in the data of Fig. 2 however suggests a smaller chemical shift of the individual C  $1s$  contributions as compared to the N  $1s$  core level and thus a strong nitrogen character of the LUMO of  $\text{Alq}_3$ .

## B. Valence-band spectra

In Fig. 5 we show the valence-band spectra of pristine and intercalated  $\text{Alq}_3$ . The data for pristine  $\text{Alq}_3$  are in good agreement with the literature.<sup>7,13</sup> The electronic states between the Fermi energy and 6 eV BE arise from the  $\pi$  states

that control the transport properties of Alq<sub>3</sub>. Above 6 eV BE one can see emission from the  $\sigma$ -derived states. Potassium intercalation causes the appearance of a feature in the energy gap of Alq<sub>3</sub>. This structure increases in intensity with increasing intercalation. This feature is attributed to the filling of the LUMO of Alq<sub>3</sub>. Theoretical calculations<sup>5</sup> predict that the wave function of the LUMO of Alq<sub>3</sub> and that of the singly occupied molecular orbital of K-intercalated Alq<sub>3</sub> are nearly identical. These calculations also predict an energy separation of the intercalation related feature to the HOMO of Alq<sub>3</sub> that is in good agreement with the experimental results.

Together with the core-level and work-function data discussed above, the valence-band spectra shown in Fig. 5 can be used to estimate the transport energy gap between the HOMO-derived valence and the LUMO-derived conduction band of Alq<sub>3</sub>. In the first step, we note that the energy distance of the HOMO onset and the chemical potential in pristine Alq<sub>3</sub> is 2.15 eV. We then consider the valence-band spectrum for a low-K doping level for which one can reasonably expect that the electronic levels themselves to be essentially unperturbed by doping. Now, the energy distance between the HOMO onset and the chemical potential is 3.05 eV, which is 0.9 eV greater than in the pristine case. This agrees perfectly with the upward shifts of 0.9 eV observed in the N 1s and O 1s binding energies as well with the downward shift of the work function, thus putting it beyond doubt that this shift is due to a change in the position of the chemical potential. Thus assuming a pinning of the chemical potential at the base of the LUMO of undoped Alq<sub>3</sub> for the low K-doping case, one can give the value of 3.05 eV as a lower bound for the transport gap in pristine Alq<sub>3</sub>. We emphasize that this figure is a lower bound, both pinning of the chemical potential at in-gap impurity states and the presence of electronic-correlation effects would mean that the true transport gap would be greater than 3.05 eV. Nevertheless, even this lower-bound value contrasts with that observed in excitation measurements. The inset to Fig. 5 shows the results of electron energy-loss investigations of Alq<sub>3</sub> carried out in transmission. The quantity measured (the loss function) is related to the electronic excitations of the system and shows an onset at 2.7 eV, in agreement with optical absorption studies.<sup>14</sup> Thus, the difference between the optical gap and the (lower bound) transport gap derived here of 0.35 eV indicates the excitonic nature of the excitations giving rise to the measured optical gap, and gives a lower estimate for the binding energy of an electron-hole pair (exciton) in solid Alq<sub>3</sub>, in qualitative agreement with recently reported results of a combined PES-IPES study.<sup>15</sup>

We stress that the difference between the two sets of gap measurements demonstrates anew that optical studies are *not* suitable to probe the transport-relevant energy gap of organic semiconductors such as Alq<sub>3</sub>. Despite this, the excitonic, optical gap value continues to be used in energy level schemes designed to explain transport data.<sup>16,17</sup>

From Fig. 5 it is also clear that none of the intercalated films are metallic as there is no emission from the Fermi level independent of the intercalation level. The binding energy of the intercalation related feature is about 2.5 eV and its separation from the former Alq<sub>3</sub> HOMO is about 1.5 eV. In view of the energy gap discussed above, these numbers show that intercalation with potassium leads to the formation of significantly relaxed electronic levels in Alq<sub>3</sub>. This energy relaxation is most probably due to a combination of two effects. First, the addition of electrons to molecular orbitals usually causes a structural relaxation of the molecules and thus a energy shift of the electronic levels. This is also expected in the case of Alq<sub>3</sub>.<sup>5,6</sup> Second, intercalation means the introduction of counterions into the structure that guarantee the charge balance. These counterions now induce an impurity potential for the electronic states, especially concerning the loosely bound valence electrons. We thus attribute the considerable energy relaxation of the Alq<sub>3</sub> LUMO upon intercalation partly to this effect. This conclusion is in agreement with previous studies of the impact of alkali ions on the electronic structure of intercalated oligomers<sup>5,6,18-20</sup> and questions the interpretation of intercalated-induced features on the basis of polarons or bipolarons alone.

#### IV. SUMMARY

We have presented a photoemission study of potassium-intercalated Alq<sub>3</sub> films as a function of the intercalation level, which reaches its maximum at K<sub>3</sub>Alq<sub>3</sub>. Our data indicate that the wave function of the lowest unoccupied molecular orbital of Alq<sub>3</sub> is composed of both carbon and nitrogen 2p states. Intercalation leads to a rigid shift of all electronic levels consistent with a constant ionization potential for all states. From this shift at a low K-doping level we have obtained an estimate of the lower limit of the transport energy gap of pristine Alq<sub>3</sub> (3.05 eV), which is significantly larger than the gap observed with absorption or excitation techniques (2.7 eV). Consequently, the optical excitation across the energy gap in Alq<sub>3</sub> is excitonic with an exciton binding energy of at least 0.35 eV. This not only implies a singlet-triplet splitting of the gap excitation, but also invalidates approaches where the optical gap is used to derive transport properties such as electron-injection barriers across a metal-Alq<sub>3</sub> interface. Finally, intercalation with potassium at a higher level causes a considerable relaxation of the electronic states of Alq<sub>3</sub> that is due to both structural modifications of the molecule and the impact of the alkali counter ions.

#### ACKNOWLEDGMENTS

This work was supported by the BMBF under 05 SF8 BD 11. We thank R. Hübel and D. Müller for technical support.

- <sup>1</sup>R.H. Friend, R.W. Gymer, A.B. Holmes, J.H. Burroughes, R.N. Marks, C. Taliani, D.D.C. Bradley, D.A. dos Santos, J.L. Brédas, M. Lögdlund, and W.R. Salaneck, *Nature (London)* **397**, 121 (1999).
- <sup>2</sup>V.E. Choong, M.G. Mason, C.W. Tang, and Y. Gao, *Appl. Phys. Lett.* **72**, 2689 (1998).
- <sup>3</sup>A. Rajagopal and A. Kahn, *J. Appl. Phys.* **84**, 355 (1998).
- <sup>4</sup>M. Probst and R. Haight, *Appl. Phys. Lett.* **70**, 11 (1997).
- <sup>5</sup>N. Johansson, T. Osada, S. Stafstöm, W.R. Salaneck, V. Parente, D.A. dos Santos, X. Crispin, and J.L. Brédas, *J. Chem. Phys.* **111**, 2157 (1999).
- <sup>6</sup>A. Curioni and W. Andreoni, *J. Am. Chem. Soc.* **121**, 8216 (1999).
- <sup>7</sup>R. Treusch, F.J. Himpsel, S. Kakar, L.J. Terminello, C. Heske, T. van Buuren, V.V. Dinh, H.W. Lee, K. Pakbaz, G. Fox, and I. Jimenez, *J. Appl. Phys.* **86**, 88 (1999).
- <sup>8</sup>M. P. Seah and W. A. Dench, *Surf. Interface Anal.* **1**, 1 (1976).
- <sup>9</sup>J.F. Moulder, W.F. Stickle, P.E. Sobol, and K.D. Bomben, *Handbook of X-ray Photoelectron Spectroscopy* (Perkin Elmer Corporation, 1992), pp. 252 ff.
- <sup>10</sup>*CRC-Handbook of Chemistry and Physics*, 75th ed., pp. 112 f. (CRC, Cleveland, OH, 1994).
- <sup>11</sup>A. Curioni, W. Andreoni, R. Treusch, F.J. Himpsel, E. Haskal, P. Seidler, C. Heske, S. Kakar, T. van Buuren, and L.J. Terminello, *Appl. Phys. Lett.* **72**, 1575 (1998).
- <sup>12</sup>D.M. Poirier, D.W. Owens, and J.H. Weaver, *Phys. Rev. B* **51**, 1830 (1995).
- <sup>13</sup>K. Sugiyama, D. Yoshimura, T. Miyamae, T. Miyazaki, H. Ishij, Y. Ouchi, and K. Seki, *J. Appl. Phys.* **83**, 4928 (1998).
- <sup>14</sup>F. Rohlfing, T. Yamada, and T. Tsutsui, *J. Appl. Phys.* **86**, 4978 (1999).
- <sup>15</sup>I.G. Hill, A. Kahn, Z.G. Soos, and R.A. Pascal, Jr., *Chem. Phys. Lett.* **327**, 181 (2000).
- <sup>16</sup>S.T. Lee, Y.M. Wang, X.Y. Hou, and C.W. Tang, *Appl. Phys. Lett.* **74**, 670 (1999).
- <sup>17</sup>See, for example, K. Tada, M. Onoda, H. Nakayama, and K. Yoshino, *Synth. Met.* **102**, 982 (1999); D. Yoshimura, T. Yokoyama, E. Ito, H. Ishii, Y. Ouchi, S. Hasegawa, and K. Seki, *ibid.* **102**, 1144 (1999).
- <sup>18</sup>M. Lögdlund, P. Dannetun, C. Fredriksson, W.R. Salaneck, and J.L. Brédas, *Phys. Rev. B* **53**, 16 327 (1996).
- <sup>19</sup>S. Irle and H. Lischka, *J. Chem. Phys.* **107**, 3021 (1997).
- <sup>20</sup>N. Koch, A. Rajagopal, E. Zojer, J. Ghijsen, X. Crispin, G. Pourtois, J.-L. Brédas, R.L. Johnson, J.-J. Pireaux, and G. Leising, *Surf. Sci.* **454-456**, 1000 (2000).